

Super-Reflection in Fluid Discs: Corotation Amplifier, Corotation Resonance, Rossby Waves, and Overstable Modes

David Tsang^{1,2*} and Dong Lai^{1*}

¹*Center for Radiophysics and Space Research, Department of Astronomy, Cornell University, Ithaca, NY 14853, USA*

²*Department of Physics, Cornell University, Ithaca, NY 14853, USA*

7 November 2021

ABSTRACT

In differentially rotating discs with no self-gravity, density waves cannot propagate around the corotation, where the wave pattern rotation speed equals the fluid rotation rate. Waves incident upon the corotation barrier may be super-reflected (commonly referred to as corotation amplifier), but the reflection can be strongly affected by wave absorptions at the corotation resonance/singularity. The sign of the absorption is related to the Rossby wave zone very near the corotation radius. We derive the explicit expressions for the complex reflection and transmission coefficients, taking into account wave absorption at the corotation resonance. We show that for generic discs, this absorption plays a much more important role than wave transmission across the corotation barrier. Depending on the sign of the gradient of the vortensity of the disc, $\zeta = \kappa^2/(2\Omega\Sigma)$ (where Ω is the rotation rate, κ is the epicyclic frequency, and Σ is the surface density), the corotation resonance can either enhance or diminish the super-reflectivity, and this can be understood in terms of the location of the Rossby wave zone relative to the corotation radius. Our results provide the explicit conditions (in terms of disc thickness, rotation profile and vortensity gradient) for which super-reflection can be achieved. Global overstable disc modes may be possible for discs with super-reflection at the corotation barrier.

Key words: accretion, accretion discs – hydrodynamics – waves – instabilities

1 INTRODUCTION

Differentially rotating fluid discs, ubiquitous in astrophysics, are known to exhibit rich dynamics and possible instabilities (e.g. Papaloizou & Lin 1995; Balbus & Hawley 1998). While local instabilities, such as Rayleigh’s centrifugal instability (for discs with specific angular momentum decreasing outwards), gravitational instability (for self-gravitational discs with too large a surface density, or more precisely, Toomre $Q \lesssim 1$), and magnetorotational instability (for discs with a sub-thermal magnetic field), are well understood (at least in the linear regime), global effects and instabilities are more subtle, since they involve couplings and feedbacks of fluid at different locations (see Goldreich 1988 for an introduction/review). A well-known example is the corotation amplifier (e.g. Mark 1976; Narayan, Goldreich & Goodman 1987), which arises from the interaction across the corotation between waves carrying opposite signs of angular momentum. Much stronger corotation amplifications (WASER – wave amplification by the stimulated emission of radiation, and SWING amplifiers) can be achieved for self-gravitating discs (e.g., Goldreich & Lynden-Bell 1965; Julian & Toomre 1966; Lin & Lau 1975; see Shu 1992 for a review). Another well-known example is the Papaloizou-Pringle instability in finite accretion tori (confined between two free surfaces), in which coupling between waves inside the corotation with those outside, combined with reflecting inner and outer boundaries, leads to violent overstable modes (Papaloizou & Pringle 1984; Goldreich et al. 1986). Recent works on global disc instabilities include the

* Email: dtsang@astro.cornell.edu; dong@astro.cornell.edu

Rossby wave instability (for discs with a strong enough density or vortensity bump; Lovelace et al. 1999; Li et al. 2000) and the accretion-ejection instability (for magnetized discs; Tagger & Pellat 1999, Tagger & Varniere 2006).

In this paper we are interested in 2D fluid discs without self-gravity and magnetic field. For disturbances of the form $e^{im\phi - i\omega t}$, where $m > 0$ and ω is the wave (angular) frequency (and thus $\omega_p = \omega/m$ is the pattern frequency), the well-known WKB dispersion relation for density waves takes the form (e.g., Shu 1992)

$$(\omega - m\Omega)^2 = \tilde{\omega}^2 = \kappa^2 + k_r^2 c^2, \quad (1)$$

where Ω is the disc rotation frequency, $\tilde{\omega} = \omega - m\Omega$ is the Doppler-shifted wave frequency, κ is the radial epicyclic frequency, k_r is the radial wavenumber, and c is the sound speed. Thus waves can propagate either inside the inner Lindblad resonance radius r_{IL} (defined by $\tilde{\omega} = -\kappa$) or outside the outer Lindblad resonance radius r_{OL} (defined by $\tilde{\omega} = \kappa$), while the region around the corotation radius r_c (set by $\tilde{\omega} = 0$) between r_{IL} and r_{OL} is evanescent. Since the wave inside r_{IL} has pattern speed ω_p smaller than the fluid rotation rate Ω , it carries negative wave action (or angular momentum), while the wave outside r_{OL} carries positive wave action. As a result, a wave incident from small radii toward the corotation barrier will be super-reflected, (with the reflected wave having a larger amplitude than the incident wave amplitude) if it can excite a wave on the other side of the corotation barrier. If there exists a reflecting boundary at the inner disc radius r_{in} , then a global overstable mode partially trapped between r_{in} and r_{IL} will result (see, e.g. Narayan et al. 1987 for specific examples in the shearing sheet model, and Goodman & Evans, 1999 and Shu et al. 2000 for global mode analysis of singular isothermal discs).

The simple dispersion relation (1), however, does not capture an important effect in the disc, i.e., corotation resonance or corotation singularity. Near corotation $|\tilde{\omega}| \ll \kappa$, the WKB dispersion relation for the wave is [see equation (17) below]

$$\tilde{\omega} = \frac{2\Omega k_\phi}{k_r^2 + k_\phi^2 + \kappa^2/c^2} \left(\frac{d}{dr} \ln \frac{\kappa^2}{2\Omega\Sigma} \right)_c, \quad (2)$$

where $k_\phi = m/r$ and Σ is the surface density, and the subscript “c” implies that the quantity is evaluated at $r = r_c$. The quantity

$$\zeta \equiv \frac{\kappa^2}{2\Omega\Sigma} = \frac{(\nabla \times \mathbf{u}_0) \cdot \hat{z}}{\Sigma} \quad (3)$$

is the vortensity of the (unperturbed) flow (where \mathbf{u}_0 is the flow velocity). The dispersion relation (2) describes Rossby waves, analogous to those studied in geophysics (e.g. Pedlosky 1987)¹. For $k_r^2 \gg \kappa^2/c^2$ and $k_r^2 \gg k_\phi^2$, we see that Rossby waves can propagate either outside the rotation radius r_c (when $d\zeta/dr > 0$) or inside r_c (when $d\zeta/dr < 0$). In either case, we have $k_r \rightarrow \infty$ as $r \rightarrow r_c$. This infinite wavenumber signifies wave absorption (cf. Lynden-Bell & Kalnajs 1972 in stellar dynamical context; Goldreich & Tremaine 1979 in the context of wave excitation in discs by a external periodic force; see also Kato 2003, Li et. al. 2003, and Zhang & Lai 2006 for wave absorption at the corotation in 3D discs). At corotation, the wave pattern angular speed ω/m matches Ω , and there can be efficient energy transfer between the wave and the background flow, analogous to Landau damping in plasma physics. Narayan et al. (1987) treated this effect as a perturbation of the shearing sheet model, and showed that the corotational absorption can convert neutral modes in a finite shearing sheet into growing or decaying modes. Papaloizou & Pringle (1987) used a WKB method to examine the effect of wave absorption at corotation on the nonaxisymmetric modes in an unbound (with the outer boundary extending to infinity) cylindrical torus.

In this paper, we derive explicit expressions for the complex reflection coefficient and transmission coefficient for waves incident upon the corotation barrier. We pay particular attention to the behavior of perturbations near the corotation resonance/singularity. Our general expressions include both the effects of corotation amplifier and wave absorption at corotation (which depends on $d\zeta/dr$). We show explicitly that depending on the sign of $d\zeta/dr$, the corotation resonance/singularity can either enhance or diminish the super-reflectivity, and this can be understood in terms of the location of the Rossby wave zone relative to the corotation radius.

Our paper is organized as follows. After presenting the general perturbation equations (section 2), we discuss the wave dispersion relation and propagation diagram, and derive the local solutions for the wave equation around the Lindblad resonances and corotation resonance (section 3). We then construct global WKB solution for the wave equation, and derive the wave reflection, transmission and corotational damping coefficients in section 4. An alternative derivation of the wave damping coefficient is presented in section 5. Readers not interested in technical details can skip Sections 2-5 and concentrate on Section 6, where we illustrate our results and discuss their physical interpretations. Section 6.1 contains a numerical calculation of the wave reflectivity across corotation and discusses the limitation of the WKB analysis. We discuss how global overstable modes may arise when super-reflection at the corotation is present in section 7 and conclude in section 8.

¹ A Rossby wave propagating in the Earth’s atmosphere satisfies the dispersion relation $\tilde{\omega} = (2k_\phi/k^2 R)(\partial\Omega_3/\partial\theta)$, where $k^2 = k_\phi^2 + k_r^2$, $\Omega_3 = \Omega \cos \theta$ is the projection of the rotation rate on the local surface normal vector and θ is the polar angle (co-latitude).

2 PERTURBATION EQUATIONS

We consider a geometrically thin gas disc and adopt cylindrical coordinate system (r, ϕ, z) . The unperturbed disc has an integrated surface density $\Sigma(r)$ and velocity $\mathbf{u}_0 = (0, r\Omega, 0)$. The flow is assumed to be barotropic, so that the integrated pressure P depends only on Σ . Self gravity of the disc is neglected.

The linear perturbation equations for the flow read

$$\frac{\partial}{\partial t} \delta \mathbf{u} + (\mathbf{u}_0 \cdot \nabla) \delta \mathbf{u} + (\delta \mathbf{u} \cdot \nabla) \mathbf{u}_0 = -\nabla \delta h, \quad (4)$$

$$\frac{\partial}{\partial t} \delta \Sigma + \nabla \cdot (\Sigma \delta \mathbf{u} + \mathbf{u}_0 \delta \Sigma) = 0, \quad (5)$$

where $\delta \Sigma$, $\delta \mathbf{u}$ and $\delta h = \delta P / \Sigma$ are the (Eulerian) perturbations of surface density, velocity and enthalpy, respectively. For barotropic flow, δh and $\delta \Sigma$ are related by

$$\delta h = c^2 \frac{\delta \Sigma}{\Sigma}, \quad (6)$$

where c is the sound speed, with $c^2 = dP/d\Sigma$.

We assume that the ϕ and t dependence of the perturbation are of the form

$$\delta \mathbf{u}, \delta \Sigma, \delta h \propto e^{im\phi - i\omega t}, \quad (7)$$

where m is a positive integer, and ω is the wave (angular) frequency. We presume $\omega > 0$ so that the pattern (angular) speed of the perturbation $\omega_p = \omega/m$ is positive (in the same direction as the flow rotation). Note that we usually assume ω is real, except in section 3.2 (dealing with the perturbation near corotation) where we include a small imaginary part ($\omega = \omega_r + i\omega_i$, with $\omega_i > 0$) to represent slowly growing disturbances. The perturbation equations (4)-(5) become

$$-i\tilde{\omega} \frac{\Sigma}{c^2} \delta h + \frac{1}{r} \frac{\partial}{\partial r} (\Sigma r \delta u_r) + \frac{im}{r} \Sigma \delta u_\phi = 0, \quad (8)$$

$$-i\tilde{\omega} \delta u_r - 2\Omega \delta u_\phi = -\frac{\partial}{\partial r} \delta h, \quad (9)$$

$$-i\tilde{\omega} \delta u_\phi + \frac{\kappa^2}{2\Omega} \delta u_r = -\frac{im}{r} \delta h, \quad (10)$$

where the epicyclic frequency κ is given by

$$\kappa^2 = \frac{2\Omega}{r} \frac{d}{dr} (r^2 \Omega). \quad (11)$$

Eliminating δu_r and δu_ϕ from equations (8)-(10), we obtain a standard second-order differential equation governing δh (e.g., Goldreich & Tremaine 1979):

$$\left[\frac{d^2}{dr^2} - \frac{d}{dr} \left(\ln \frac{D}{r\Sigma} \right) \frac{d}{dr} - \frac{2m\Omega}{r\tilde{\omega}} \left(\frac{d}{dr} \ln \frac{\Omega\Sigma}{D} \right) - \frac{m^2}{r^2} - \frac{D}{c^2} \right] \delta h = 0, \quad (12)$$

where

$$D \equiv \kappa^2 - \tilde{\omega}^2 = \kappa^2 - (\omega - m\Omega)^2. \quad (13)$$

Defining

$$S = D/(r\Sigma), \quad \eta = S^{-1/2} \delta h, \quad (14)$$

we can rewrite (12) as a wave equation

$$\left[\frac{d^2}{dr^2} - \frac{D}{c^2} - \frac{m^2}{r^2} - \frac{2m\Omega}{r\tilde{\omega}} \left(\frac{d}{dr} \ln \frac{\Omega\Sigma}{D} \right) - S^{1/2} \frac{d^2}{dr^2} S^{-1/2} \right] \eta = 0. \quad (15)$$

This is our basic working equation.

3 PROPAGATION DIAGRAM AND LOCAL SOLUTIONS NEAR RESONANCES

Consider local free wave solution of the form

$$\delta h \propto \exp \left[i \int^r k_r(s) ds \right]. \quad (16)$$

For $|k_r r| \gg m$ and away from the $D = 0$ region, we find from equation (15)

$$k_r^2 + \frac{D}{c^2} + \frac{2m\Omega}{r\tilde{\omega}} \left(\frac{d}{dr} \ln \frac{\Omega\Sigma}{D} \right) \simeq 0. \quad (17)$$

This is the general WKB dispersion relation. Away from the region where $\tilde{\omega} = 0$, this reduces to the well-known result $k_r^2 \simeq -D/c^2$ [equation (1)]; in the vicinity of $\tilde{\omega} = 0$ this describes local Rossby waves, with [see equations (2)-(3)]

$$\tilde{\omega} \simeq \frac{2m\Omega}{rk_r^2} \left(\frac{d \ln \zeta}{dr} \right)_c. \quad (18)$$

Before studying global solutions to the wave equation (12) or (15), it is useful to consider the special resonant locations in the disc. These can be recognized by investigating the singular points and turning points of the wave equation (12) or (15), or by examining the characteristics of the dispersion relation (17). The special radii are

(i) Lindblad resonances (LRs), where $D = 0$ or $\tilde{\omega}^2 = \kappa^2$, including the outer Lindblad resonance (OLR) at $\tilde{\omega} = \kappa$ and the inner Lindblad resonance (ILR) at $\tilde{\omega} = -\kappa$. The LR is an apparent singularity of equation (12) or (15) – all physical quantities are finite at $D = 0$. The LR is a turning point at which wave trains are reflected or transmitted. In the presence of an external force, waves are launched from LR.

(ii) Corotation resonance (CR), where $\tilde{\omega} = 0$. In general, the CR is a singular point of the wave equation except in the special case of $d\zeta/dr = 0$ at corotation. Some physical quantities (e.g., azimuthal velocity perturbation) are divergent at corotation. Physically, this singularity signifies that a steady emission or absorption of wave action may occur there.

From equation (15), we define the effective potential for wave propagation by

$$\begin{aligned} V_{\text{eff}}(r) &= \frac{D}{c^2} + \frac{m^2}{r^2} + \frac{2m\Omega}{r\tilde{\omega}} \left(\frac{d}{dr} \ln \frac{\Omega\Sigma}{D} \right) + S^{1/2} \frac{d^2}{dr^2} S^{-1/2} \\ &= V_{\text{eff},0}(r) + \Delta V_{\text{eff}}(r), \end{aligned} \quad (19)$$

where

$$V_{\text{eff},0}(r) = \frac{D}{c^2} + \frac{m^2}{r^2} - \frac{2m\Omega}{r\tilde{\omega}} \left(\frac{d}{dr} \ln \zeta \right), \quad (20)$$

$$\Delta V_{\text{eff}}(r) = -\frac{2m\Omega}{r\tilde{\omega}} \frac{d}{dr} \ln \frac{D}{\kappa^2} + S^{1/2} \frac{d^2}{dr^2} S^{-1/2}. \quad (21)$$

Clearly, wave propagation is possible only in the region where $V_{\text{eff}}(r) < 0$. Figures 1-3 depict the wave propagation diagrams for the cases of $(d\zeta/dr)_c = 0$, < 0 and > 0 , respectively. We are interested in the parameter regime $c/(r\Omega) \ll 1$ and m is of order unity. Note that the apparent singularity in $\Delta V_{\text{eff}}(r)$ at $D = 0$ can be eliminated by analysing the wave solution around the LR (see section 3.1 below). Thus we also show $V_{\text{eff},0}(r)$ in Figs. 1-3.

We now consider the behaviors of the perturbations around the LR and CR.

3.1 Solution Around Lindblad Resonances

Equation (15) has an apparent singularity at the LR, where $D \rightarrow 0$. For concreteness we will explicitly examine the outer Lindblad resonance (OLR); a similar solution can be found for the inner Lindblad resonance (ILR).

In the vicinity of the OLR, equation (15) becomes

$$\frac{d^2}{dr^2} \eta + \left(k^2 - k \frac{d^2}{dr^2} \frac{1}{k} + \frac{4m\Omega}{r\tilde{\omega}k} \frac{dk}{dr} \right) \eta = 0, \quad (22)$$

where $k^2 \equiv -D/c^2$. The last term inside (\dots) is smaller than the second term and will be neglected. Changing the independent variable from r to the dimensionless integrated phase

$$z = \int_{r_{\text{OL}}}^r k dr, \quad (23)$$

we have

$$V'' + \left[\frac{k''}{2k} - \frac{3}{4} \left(\frac{k'}{k} \right)^2 + 1 \right] V = 0, \quad (24)$$

where

$$V = \sqrt{k} \eta = \sqrt{\frac{k}{S}} \delta h, \quad (25)$$

and the prime denotes differentiation with respect to z . Note that near OLR, $k^2 \simeq C(r - r_{\text{OL}})$, with $C = (-c^{-2}dD/dr)_{\text{OL}} > 0$ a constant, we have

$$z = \begin{cases} \frac{2}{3} C^{1/2} (r - r_{\text{OL}})^{3/2} & \text{for } r > r_{\text{OL}} \\ \frac{2}{3} C^{1/2} (r_{\text{OL}} - r)^{3/2} e^{i3\pi/2} & \text{for } r < r_{\text{OL}} \end{cases} \quad (26)$$

We can then express k in terms of z as

$$k = \left(\frac{3}{2} C \right)^{1/3} z^{1/3}. \quad (27)$$

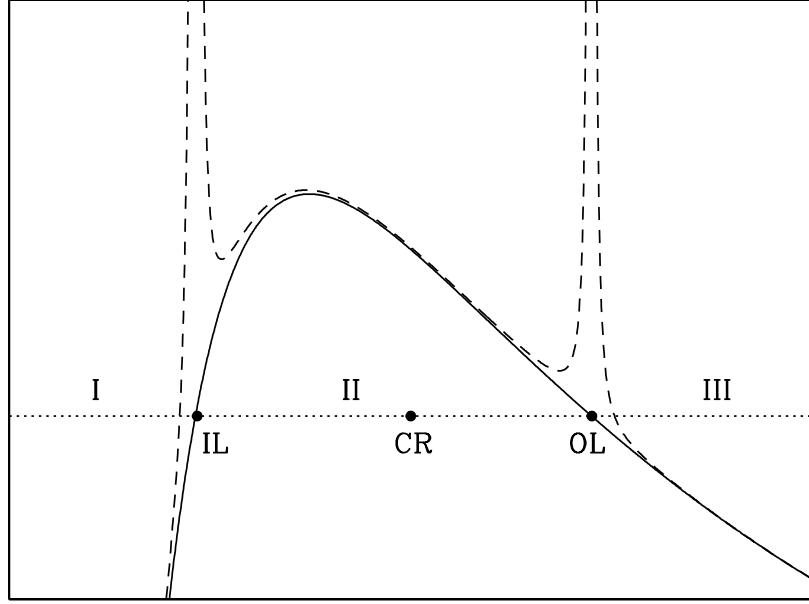


Figure 1. Wave propagation diagram in Keplerian discs: A sketch of the effective potential $V_{\text{eff},0}(r)$ (solid line) and $V_{\text{eff}}(r)$ (dashed line) as a function of r , for the case of $(d\zeta/dr)_c = 0$. Waves can propagate only in the region where $V_{\text{eff}}(r) < 0$, i.e., where the curves are below the dotted line. The three special locations are denoted by IL (Inner Lindblad Resonance), OL (Outer Lindblad Resonance) and CR (Corotation Resonance). The divergence in the $V_{\text{eff}}(r)$ curve around IL and OL represents an apparent singularity.

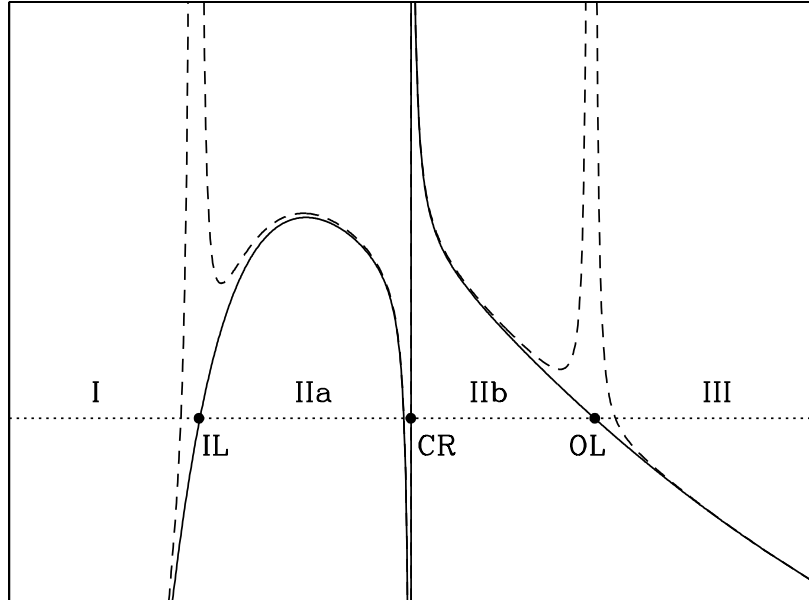


Figure 2. Same as Fig. 1, except for the case of negative vortensity gradient, $(d\zeta/dr)_c < 0$ (or $\nu < 0$). Note the CR represents a singularity, and the Rossby wave zone lies inside the corotation radius.

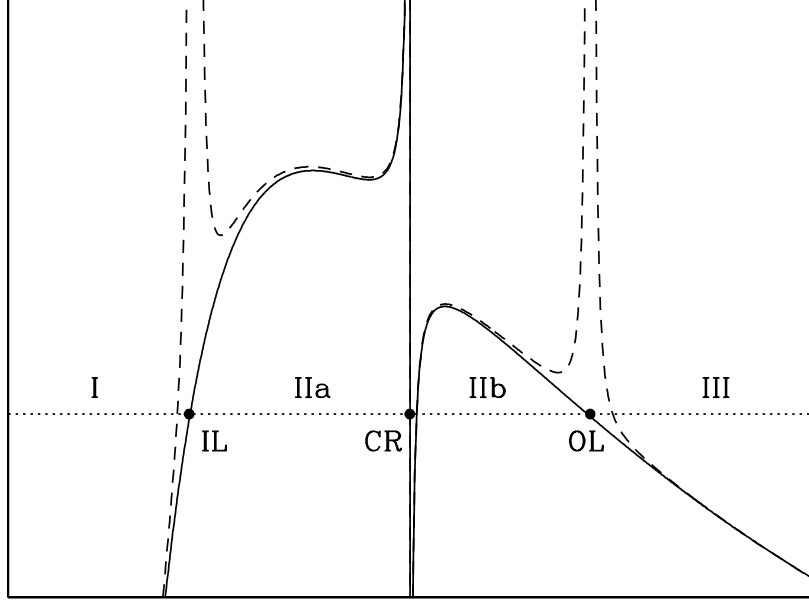


Figure 3. Same as Fig. 1, except for the case of positive vortensity gradient, $(d\zeta/dr)_c > 0$ (or $\nu > 0$), for which the Rossby wave zone lies outside the corotation radius.

Using equation (27) in equation (24) we have

$$V'' + \left(1 - \frac{7}{36z^2}\right) V = 0. \quad (28)$$

Equation (28) has two independent solutions in terms of Bessel function (Abramowitz & Stegun 1964)

$$V = \sqrt{z} J_{\pm 2/3}(z) = \frac{1}{(12z)^{1/6}} \left[\pm \sqrt{3} \text{Ai}'(-Z) + \text{Bi}'(-Z) \right], \quad (29)$$

where $Z = (3z/2)^{2/3}$, and Ai' , Bi' are the derivatives of the Airy functions. Instead of using $\sqrt{z} J_{\pm 2/3}(z)$, we can construct two linearly independent solutions for η in a form convenient for asymptotic matching:

$$\eta_1 = -\left(\frac{\pi}{k}\right)^{1/2} \left(\frac{2}{3z}\right)^{1/6} \text{Ai}'(-Z) \sim \begin{cases} \frac{1}{\sqrt{k}} \cos(z + \pi/4) & \text{for } |z| \gg 1 \text{ and } \arg(z) = 0 \\ \frac{1}{2\sqrt{k}} \exp(-|z|) & \text{for } |z| \gg 1 \text{ and } \arg(z) = 3\pi/2 \end{cases} \quad (30)$$

$$\eta_2 = \left(\frac{\pi}{k}\right)^{1/2} \left(\frac{2}{3z}\right)^{1/6} \text{Bi}'(-Z) \sim \begin{cases} \frac{1}{\sqrt{k}} \sin(z + \pi/4) & \text{for } |z| \gg 1 \text{ and } \arg(z) = 0 \\ \frac{1}{\sqrt{k}} \exp(|z|) & \text{for } |z| \gg 1 \text{ and } \arg(z) = 3\pi/2 \end{cases} \quad (31)$$

where \sim indicates asymptotic expansions. This gives the connection formulae for the enthalpy perturbation at the OLR²:

$$\delta h_1 \sim \begin{cases} \frac{1}{2} \sqrt{S/k} \exp\left(-\int_r^{r_{\text{OL}}} |k| dr\right) & \text{for } r \ll r_{\text{OL}} \\ \sqrt{S/k} \cos\left(\int_{r_{\text{OL}}}^r k dr + \pi/4\right) & \text{for } r \gg r_{\text{OL}} \end{cases} \quad (32)$$

$$\delta h_2 \sim \begin{cases} \sqrt{S/k} \exp\left(\int_r^{r_{\text{OL}}} |k| dr\right) & \text{for } r \ll r_{\text{OL}} \\ \sqrt{S/k} \sin\left(\int_{r_{\text{OL}}}^r k dr + \pi/4\right) & \text{for } r \gg r_{\text{OL}} \end{cases} \quad (33)$$

² The usage here of \gg is used as a shorthand for the range of validity for an asymptotic expansion of a local solution. The fitting formulae are to be used far enough away from the resonances so that the asymptotic expansion is valid, but close enough that the local approximation made in (22) holds.

The connection formulae for ILR can be similarly derived:³

$$\delta h_1 \sim \begin{cases} \frac{1}{2} \sqrt{S/k} \exp\left(-\int_{r_{\text{IL}}}^r |k| dr\right) & \text{for } r \gg r_{\text{IL}} \\ \sqrt{S/k} \cos\left(\int_{r_{\text{IL}}}^r k dr + \pi/4\right) & \text{for } r \ll r_{\text{IL}} \end{cases} \quad (34)$$

$$\delta h_2 \sim \begin{cases} \sqrt{S/k} \exp\left(\int_{r_{\text{IL}}}^r |k| dr\right) & \text{for } r \gg r_{\text{IL}} \\ \sqrt{S/k} \sin\left(\int_{r_{\text{IL}}}^r k dr + \pi/4\right) & \text{for } r \ll r_{\text{IL}} \end{cases} \quad (35)$$

3.2 Solution Around Corotation Radius

In the vicinity of the corotation radius r_c , we can rewrite (15) dropping the m^2/r^2 and S terms compared to the singular term proportional to $1/\tilde{\omega}$, giving

$$\left[\frac{d^2}{dr^2} - \tilde{k}^2 + \frac{2}{q} \left(\frac{d}{dr} \ln \frac{\kappa^2}{\Omega \Sigma} \right)_c \frac{1}{r - R_c} \right] \eta = 0, \quad (36)$$

where

$$\tilde{k}^2 \equiv \frac{D}{c^2}, \quad q \equiv - \left(\frac{d \ln \Omega}{d \ln r} \right)_c, \quad R_c \equiv r_c - i \frac{r_c \omega_i}{q \omega_r}. \quad (37)$$

Here we have introduced a small imaginary part to the wave frequency, so that $\omega = \omega_r + i\omega_i$. To study the response of the disc to a slowly increasing perturbation, we require $\omega_i > 0$. Defining

$$x = \int_{r_c}^r 2\tilde{k} dr, \quad \eta = \frac{1}{\sqrt{\tilde{k}}} \psi, \quad (38)$$

and recognizing that \tilde{k} can be treated as a constant around corotation, we have

$$\frac{d^2}{dx^2} \psi + \left(-\frac{1}{4} + \frac{\nu}{x + i\epsilon} \right) \psi = 0 \quad (39)$$

where $\epsilon = 2\tilde{k}r_c\omega_i/(q\omega_r)$ and

$$\nu = \frac{1}{q\tilde{k}} \left(\frac{d}{dr} \ln \frac{\kappa^2}{\Omega \Sigma} \right)_c = \left(\frac{c}{q\kappa} \frac{d}{dr} \ln \zeta \right)_c. \quad (40)$$

In equation (39) $\epsilon > 0$, consistent with the initial value problem in which the perturbation is gradually turned on starting from $t = -\infty$. The parameter ν determines the width of the Rossby wave region, $\Delta r_R = (2c/\kappa)|\nu|$. For $d \ln \zeta / dr \sim 1/r$, we have $|\nu| \sim (H/r)_c$ (H is the disc scale height).⁴

Equation (39) is the differential equation for the Whittaker function in complex variable $z = x + i\epsilon$ with index $1/2$ (Abramowitz & Stegun 1964). The two linearly independent solutions convenient for the connection are

$$\psi_- = W_{\nu, 1/2}(z), \quad \psi_+ = e^{-i\pi\nu} W_{-\nu, 1/2}(ze^{-i\pi}) + \frac{1}{2} T_0 W_{\nu, 1/2}(z), \quad (41)$$

where T_0 is the Stokes multiplier defined below, and z is defined in the complex plane so that $\arg(z)$ ranges from 0 to π . The particular linear combinations of Whittaker functions in (41) are chosen so that appropriate asymptotic expansions can be obtained. To obtain these asymptotic expansions and the connection formulae around the corotation, one must carefully consider the Stokes phenomenon, which alters the form of the asymptotic expansion of a function depending on the position of z in the complex plane. Since the appropriate asymptotic expansions (which connect the solution $W_{\pm\nu, 1/2}$ analytically in different regions of the complex plane) are not readily available, we relegate the discussion of the Stokes phenomenon for the Whittaker function around the corotation to Appendix A⁵. The resulting connection formulae are

$$\delta h_- \sim \begin{cases} \sqrt{S/k} \exp\left(-\int_{r_c}^r \tilde{k} dr\right) & \text{for } r \gg r_c \\ \sqrt{S/k} e^{i\pi\nu} \exp\left(+\int_{r_c}^r \tilde{k} dr\right) + \sqrt{S/k} \frac{T_1}{2} e^{-i\pi\nu} \exp\left(-\int_{r_c}^r \tilde{k} dr\right) & \text{for } r \ll r_c \end{cases} \quad (42)$$

$$\delta h_+ \sim \begin{cases} \sqrt{S/k} \exp\left(+\int_{r_c}^r \tilde{k} dr\right) & \text{for } r \gg r_c \\ \sqrt{S/k} \frac{T_1}{2} e^{i\pi\nu} \exp\left(+\int_{r_c}^r \tilde{k} dr\right) + \sqrt{S/k} \left(1 + \frac{T_1 T_0}{4}\right) e^{-i\pi\nu} \exp\left(-\int_{r_c}^r \tilde{k} dr\right) & \text{for } r \ll r_c \end{cases} \quad (43)$$

³ Note that for the ILR, k is real for $r < r_{\text{IL}}$ and imaginary for $r > r_{\text{IL}}$, while for the OLR, k is real for $r > r_{\text{OL}}$ and imaginary for $r < r_{\text{OL}}$.

⁴ Note that the WKB wavenumber k_r in the Rossby region ranges from ∞ (at $r = r_c$) to H^{-1} (at $r \sim r_c \pm \Delta r_R$) [see equation (18)] while the width of the region is of order H^2/r for most Keplerian discs. Free Rossby waves tend to be sheared away by differential rotation (Tagger 2001).

⁵ The Stokes phenomenon is present in our Lindblad resonance analysis as well, as we see, for example, the asymptotic expansion for $Bi'(-(3z/2)^{2/3})$ takes the form $e^{+|z|}$ for $\arg(z) = 3\pi/2$ but $\sin(z + \pi/4)$ (as opposed to e^{iz}) for $\arg(z) = 0$. The resulting connection formulae are well known for the Airy functions.

where T_0 and T_1 are the Stokes multipliers,

$$T_0 = \frac{2\pi i}{\Gamma(\nu)\Gamma(1+\nu)}, \quad T_1 = \frac{2\pi i e^{i2\pi\nu}}{\Gamma(-\nu)\Gamma(1-\nu)}. \quad (44)$$

Note that for $|\nu| \ll 1$, $[\Gamma(\pm\nu)]^{-1} = \pm\nu + \gamma\nu^2 + \dots$, where $\gamma = 0.5772$ is the Euler constant.

4 GLOBAL WKB SOLUTIONS AND CALCULATION OF REFLECTIVITY

In this section we consider a wave train which approaches corotation from small radii ($r \ll r_{\text{IL}}$). Its propagation is impeded by the potential barrier between r_{IL} and r_{OL} . The incident wave is partially transmitted beyond the OLR and a reflected wave propagates from the ILR toward small radii. We will derive the explicit expressions for the (complex) reflection coefficient \mathcal{R} and transmission coefficient \mathcal{T} .

From the dispersion relation [equation (1), or equation (17) away from corotation], we find that the radial group velocity of the waves is

$$c_g = \frac{d\omega}{dk_r} = \frac{k_r c^2}{\tilde{\omega}(1 - \kappa^2/\tilde{\omega}^2)}. \quad (45)$$

Thus the sign of c_g/c_p (where $c_p = \omega/k_r$ is the phase velocity) is positive for $r > r_{\text{OL}}$ and negative for $r < r_{\text{IL}}$. This implies that in the $r > r_{\text{OL}}$ region, the outgoing (transmitted) wave has the form $\exp(i \int^r k_r dr)$ (assuming $k_r > 0$). In the $r < r_{\text{IL}}$ region, the incident wave (propagating from small radii toward corotation) has the form $\exp(-i \int^r k_r dr)$, while the reflected wave has the form $\exp(i \int^r k_r dr)$.

A well-known property of density waves is that for $r < r_{\text{IL}}$ the wave carries negative energy (or angular momentum), while for $r > r_{\text{OL}}$ the wave carries positive energy. An incident wave $\exp(-i \int^r k_r dr)$, carrying energy of the amount (-1) , will give rise to a reflected wave $\mathcal{R} \exp(i \int^r k_r dr)$ and a transmitted wave $\mathcal{T} \exp(i \int^r k_r dr)$. Let \mathcal{D}_c be the energy dissipated at the corotation. Then energy conservation gives $-1 = (-1)|\mathcal{R}|^2 + |\mathcal{T}|^2 + \mathcal{D}_c$, or

$$|\mathcal{R}|^2 = 1 + |\mathcal{T}|^2 + \mathcal{D}_c. \quad (46)$$

Because of the singularity at corotation and the associated energy absorption, we first consider the simple case where the corotation singularity is neglected (section 4.1) before examining the general case (section 4.2).

4.1 Neglecting Corotation Singularity: Corotation Amplifier

Here we consider the case where the vortensity has zero slope at corotation, i.e., $(d\zeta/dr)_c = 0$. This would occur for disc models where the specific angular momentum $r^2\Omega$ is constant (as in the original Papaloizou & Pringle 1984 analysis), or for shearing sheet approximation (as in Narayan et al. 1987). In this case, there is no corotation singularity and no absorption of wave energy, and we always obtain super-reflection

$$|\mathcal{R}|^2 = 1 + |\mathcal{T}|^2 > 1. \quad (47)$$

This is the essence of the corotation amplifier.

To derive the complex \mathcal{R} and \mathcal{T} , we assume that the outgoing wave in the $r > r_{\text{OL}}$ region (region III in Fig. 1) is given by [see eqs. (32)-(33)]

$$\delta h = \sqrt{S/k} \exp\left(i \int_{r_{\text{OL}}}^r k dr + \frac{\pi}{4}\right), \quad (48)$$

where $k^2 \equiv -D/c^2$. The connection formulae (32)-(33) then give for the evanescent zone (region II in Fig. 1):

$$\begin{aligned} \delta h &\simeq \frac{\sqrt{S/k}}{2} \exp\left(-\int_r^{r_{\text{OL}}} |k| dr\right) + i\sqrt{S/k} \exp\left(\int_r^{r_{\text{OL}}} |k| dr\right) \\ &= \frac{\sqrt{S/k}}{2} \exp(-\Theta_{\text{II}}) \exp\left(\int_{r_{\text{IL}}}^r |k| dr\right) + i\sqrt{S/k} \exp(+\Theta_{\text{II}}) \exp\left(-\int_{r_{\text{IL}}}^r |k| dr\right) \end{aligned} \quad (49)$$

where

$$\Theta_{\text{II}} = \int_{r_{\text{IL}}}^{r_{\text{OL}}} |k| dr = \int_{r_{\text{IL}}}^{r_{\text{OL}}} \frac{\sqrt{|D|}}{c} dr. \quad (50)$$

Using the connection formulae at ILR [eqs. (34)-(35)], we find that for $r < r_{\text{IL}}$ (region I in Fig. 1)

$$\delta h \simeq \frac{\sqrt{S/k}}{2} e^{-\Theta_{\text{II}}} \sin\left(\int_r^{r_{\text{IL}}} k dr + \frac{\pi}{4}\right) + i2\sqrt{S/k} e^{\Theta_{\text{II}}} \cos\left(\int_r^{r_{\text{IL}}} k dr + \frac{\pi}{4}\right). \quad (51)$$

Expressing this in terms of traveling waves, and defining $y = \int_{r_{\text{IL}}}^r k dr - \pi/4$ we have

$$\delta h \simeq i\sqrt{S/k} \left[e^{-iy} \left(e^{+\Theta_{\text{II}}} - \frac{1}{4}e^{-\Theta_{\text{II}}} \right) + e^{+iy} \left(e^{\Theta_{\text{II}}} + \frac{1}{4}e^{-\Theta_{\text{II}}} \right) \right]. \quad (52)$$

Thus the reflection coefficient is

$$\mathcal{R} = \frac{e^{\Theta_{\text{II}}} + \frac{1}{4}e^{-\Theta_{\text{II}}}}{e^{\Theta_{\text{II}}} - \frac{1}{4}e^{-\Theta_{\text{II}}}}. \quad (53)$$

Comparing equation (52) with equation (48), we obtain the transmission coefficient

$$\mathcal{T} = \frac{-i}{e^{+\Theta_{\text{II}}} - \frac{1}{4}e^{-\Theta_{\text{II}}}}. \quad (54)$$

As expected, $|\mathcal{R}|^2 = 1 + |\mathcal{T}|^2 > 1$.

4.2 Including Corotation Singularity

As noted before, for discs with nonzero vortensity gradient ($d\zeta/dr \neq 0$), the singularity at corotation implies the absorption of wave energy (or angular momentum). Similar situations occur in geophysical wave systems (Dickenson 1968) and for waves in plasmas (Landau damping). In Appendix B, we discuss the toy problem of resonant tunneling which shares the similar energy absorption feature as the corotation singularity. Previous works on global modes in disc tori (e.g. Papaloizou & Pringle 1987; Goldreich et al. 1986; Narayan et al. 1987) suggest that the sign of $d\zeta/dr$ determines whether the singularity acts to stabilize or destabilize a global mode. Here we derive the explicit expression for the reflectivity and the related source term \mathcal{D}_c .

As in section 4.1, we assume an outgoing wave in Region III, and the connection formulae at the OLR then give for Region IIb of Fig. 2 or Fig. 3

$$\delta h \simeq \frac{\sqrt{S/k}}{2} \exp(-\Theta_{\text{IIb}}) \exp\left(\int_{r_c}^r |k| dr\right) + i\sqrt{S/k} \exp(+\Theta_{\text{IIb}}) \exp\left(-\int_{r_c}^r |k| dr\right), \quad (55)$$

where

$$\Theta_{\text{IIb}} = \int_{r_c}^{r_{\text{OL}}} |k| dr. \quad (56)$$

Equation (55) is the asymptotic solution away from the r_c in region IIb. The corresponding general solution around r_c is

$$\delta h = \frac{\sqrt{S/k}}{2} \exp(-\Theta_{\text{IIb}}) \psi_+(r) + i\sqrt{S/k} \exp(\Theta_{\text{IIb}}) \psi_-(r), \quad (57)$$

where ψ_+ and ψ_- are given by (41). Using equations (42) and (43) to match asymptotes over the corotation singularity, we obtain in Region IIa

$$\begin{aligned} \delta h \simeq & \left[\frac{1}{2} \exp(-\Theta_{\text{IIb}}) \left(1 + \frac{1}{4} T_0 T_1 \right) + \frac{i}{2} T_1 \exp(+\Theta_{\text{IIb}}) \right] \sqrt{S/k} e^{-i\pi\nu} \exp\left(-\int_r^{r_c} |k| dr\right) \\ & + i \left[\exp(+\Theta_{\text{IIb}}) - \frac{i}{4} T_0 \exp(-\Theta_{\text{IIb}}) \right] \sqrt{S/k} e^{i\pi\nu} \exp\left(\int_r^{r_c} |k| dr\right). \end{aligned} \quad (58)$$

Using the connection formulae at the ILR, we have for Region I:

$$\begin{aligned} \delta h \simeq & \left[\frac{1}{2} \exp(-\Theta_{\text{II}}) \left(1 + \frac{1}{4} T_0 T_1 \right) + \frac{i}{2} T_1 \exp(\Theta_{\text{IIb}} - \Theta_{\text{IIa}}) \right] \sqrt{S/k} e^{-i\pi\nu} \sin\left(\int_r^{r_{\text{IL}}} k dr + \frac{\pi}{4}\right) \\ & + 2i \left[\exp(+\Theta_{\text{II}}) - \frac{i}{4} T_0 \exp(\Theta_{\text{IIa}} - \Theta_{\text{IIb}}) \right] \sqrt{S/k} e^{i\pi\nu} \cos\left(\int_r^{r_{\text{IL}}} k dr + \frac{\pi}{4}\right) \\ = & \left[1 + \frac{1}{4} e^{-i2\pi\nu} e^{-2\Theta_{\text{II}}} \left(1 + \frac{1}{4} T_0 T_1 \right) + \frac{i}{4} T_1 e^{-i2\pi\nu} e^{-2\Theta_{\text{IIa}}} - \frac{i}{4} T_0 e^{-2\Theta_{\text{IIb}}} \right] i\sqrt{S/k} e^{\Theta_{\text{II}}} e^{i\pi\nu} e^{iy} \\ & + \left[1 - \frac{1}{4} e^{-i2\pi\nu} e^{-2\Theta_{\text{II}}} \left(1 + \frac{1}{4} T_0 T_1 \right) - \frac{i}{4} T_1 e^{-i2\pi\nu} e^{-2\Theta_{\text{IIa}}} - \frac{i}{4} T_0 e^{-2\Theta_{\text{IIb}}} \right] i\sqrt{S/k} e^{\Theta_{\text{II}}} e^{i\pi\nu} e^{-iy}, \end{aligned} \quad (59)$$

where $y = \int_{r_{\text{IL}}}^r k dr - \pi/4$ and

$$\Theta_{\text{IIa}} = \int_{r_{\text{IL}}}^{r_c} |k| dr, \quad \Theta_{\text{II}} = \Theta_{\text{IIa}} + \Theta_{\text{IIb}} = \int_{r_{\text{IL}}}^{r_{\text{OL}}} |k| dr. \quad (60)$$

The reflection coefficient and transmission coefficient are then

$$\mathcal{R} = \frac{1 + \frac{1}{4} e^{-i2\pi\nu} e^{-2\Theta_{\text{II}}} \left(1 + \frac{1}{4} T_0 T_1\right) + \frac{i}{4} T_1 e^{-i2\pi\nu} e^{-2\Theta_{\text{IIa}}} - \frac{i}{4} T_0 e^{-2\Theta_{\text{IIb}}}}{1 - \frac{1}{4} e^{-i2\pi\nu} e^{-2\Theta_{\text{II}}} \left(1 + \frac{1}{4} T_0 T_1\right) - \frac{i}{4} T_1 e^{-i2\pi\nu} e^{-2\Theta_{\text{IIa}}} - \frac{i}{4} T_0 e^{-2\Theta_{\text{IIb}}}},$$

$$= \frac{1 + \frac{1}{4} (e^{-i2\pi\nu} + \sin^2 \pi\nu) e^{-2\Theta_{\text{II}}} + \frac{\pi\nu}{2} \frac{e^{-2\Theta_{\text{IIa}}}}{(\Gamma(1-\nu))^2} - \frac{\pi\nu}{2} \frac{e^{-2\Theta_{\text{IIb}}}}{(\Gamma(1+\nu))^2}}{1 - \frac{1}{4} (e^{-i2\pi\nu} + \sin^2 \pi\nu) e^{-2\Theta_{\text{II}}} - \frac{\pi\nu}{2} \frac{e^{-2\Theta_{\text{IIa}}}}{(\Gamma(1-\nu))^2} - \frac{\pi\nu}{2} \frac{e^{-2\Theta_{\text{IIb}}}}{(\Gamma(1+\nu))^2}} \quad (61)$$

$$\mathcal{T} = \frac{-i e^{-\Theta_{\text{II}}} e^{i\pi\nu}}{1 - \frac{1}{4} e^{-i2\pi\nu} e^{-2\Theta_{\text{II}}} \left(1 + \frac{1}{4} T_0 T_1\right) - \frac{i}{4} T_1 e^{-i2\pi\nu} e^{-2\Theta_{\text{IIa}}} - \frac{i}{4} T_0 e^{-2\Theta_{\text{IIb}}}}$$

$$= \frac{-i e^{-\Theta_{\text{II}}} e^{i\pi\nu}}{1 - \frac{1}{4} (e^{-i2\pi\nu} + \sin^2 \pi\nu) e^{-2\Theta_{\text{II}}} - \frac{\pi\nu}{2} \frac{e^{-2\Theta_{\text{IIa}}}}{(\Gamma(1-\nu))^2} - \frac{\pi\nu}{2} \frac{e^{-2\Theta_{\text{IIb}}}}{(\Gamma(1+\nu))^2}} \quad (62)$$

The dissipation term due to the corotation singularity obtained from $\mathcal{D}_c = |\mathcal{R}|^2 - 1 - |\mathcal{T}|^2$ is

$$\mathcal{D}_c = \frac{\frac{\pi\nu}{2} \frac{\cos^2 \pi\nu}{(\Gamma(1+\nu))^2} e^{-2\Theta_{\text{II}} - 2\Theta_{\text{IIb}}} + \frac{2\pi\nu}{(\Gamma(1-\nu))^2} e^{-2\Theta_{\text{IIa}}}}{|1 - \frac{1}{4} (e^{-i2\pi\nu} + \sin^2 \pi\nu) e^{-2\Theta_{\text{II}}} - \frac{\pi\nu}{2} \frac{e^{-2\Theta_{\text{IIa}}}}{(\Gamma(1-\nu))^2} - \frac{\pi\nu}{2} \frac{e^{-2\Theta_{\text{IIb}}}}{(\Gamma(1+\nu))^2}|^2}. \quad (63)$$

For $|\nu| \ll 1$ equations (61) and (62) can be simplified, and we have

$$\mathcal{R} \rightarrow \frac{e^{\Theta_{\text{II}}} + \frac{1}{4} e^{-\Theta_{\text{II}}}}{e^{\Theta_{\text{II}}} - \frac{1}{4} e^{-\Theta_{\text{II}}}} + \frac{e^{+2\Theta_{\text{IIb}}} - \frac{1}{4} e^{-2\Theta_{\text{IIb}}}}{(e^{\Theta_{\text{II}}} - \frac{1}{4} e^{-\Theta_{\text{II}}})^2} \pi\nu + \mathcal{O}[\nu^2], \quad (64)$$

$$\mathcal{T} \rightarrow \frac{-i}{e^{\Theta_{\text{II}}} - \frac{1}{4} e^{-\Theta_{\text{II}}}} - \frac{i}{2} \frac{e^{\Theta_{\text{IIb}} - \Theta_{\text{IIa}}} - e^{\Theta_{\text{IIa}} - \Theta_{\text{IIb}}}}{(e^{\Theta_{\text{II}}} - \frac{1}{4} e^{-\Theta_{\text{II}}})^2} \pi\nu + \mathcal{O}[\nu^2], \quad (65)$$

$$\mathcal{D}_c \rightarrow \frac{2(e^{\Theta_{\text{II}}} + \frac{1}{4} e^{-\Theta_{\text{II}}})(e^{2\Theta_{\text{IIb}}} - \frac{1}{4} e^{-2\Theta_{\text{IIb}}}) + (e^{\Theta_{\text{IIb}} - \Theta_{\text{IIa}}} - e^{\Theta_{\text{IIa}} - \Theta_{\text{IIb}}})}{(e^{\Theta_{\text{II}}} - \frac{1}{4} e^{-\Theta_{\text{II}}})^3} \pi\nu + \mathcal{O}[\nu^2]. \quad (66)$$

Clearly, for $\nu = 0$, equations (64)-(65) reduce to (53) and (54).

5 WAVE DAMPING AT COROTATION: ALTERNATIVE CALCULATION

In the previous section we obtained the expression for the dissipation term \mathcal{D}_c at the corotation resonance using the reflection and transmission coefficients. Here we provide a more direct derivation of \mathcal{D}_c using the change of angular momentum flux across the corotation radius.

In the absence of self-gravity, the angular momentum flux carried by the waves in the disc is entirely due to advection. The time-averaged transfer rate of the z -component of angular momentum across a cylinder of radius r (in the outward direction) is given by (e.g. Goldreich & Tremaine 1979)

$$F(r) = r^2 \Sigma(r) \int_0^{2\pi} d\phi \operatorname{Re}[\delta u_r(r, \phi, t)] \operatorname{Re}[\delta u_\phi(r, \phi, t)]. \quad (67)$$

Using equations (9)-(10) to express δu_r and δu_ϕ in terms of δh , this reduces to (see Tanaka et al. 2002; Zhang & Lai 2006)

$$F(r) = \frac{\pi m r \Sigma}{D} \operatorname{Im} \left(\delta h \frac{d\delta h^*}{dr} \right). \quad (68)$$

In Region III (see Figs. 1-3) the outgoing wave has the enthalpy perturbation given by (up to a proportional constant)

$$\delta h = \sqrt{S/k} \mathcal{T} \exp \left(i \int_{r_{\text{OL}}}^r k dr + \frac{\pi}{4} \right) \quad (69)$$

Calculating the angular momentum flux (setting the incoming wave flux to 1),

$$F(r \gg r_{\text{OL}}) \simeq \pi m |\mathcal{T}|^2, \quad (70)$$

we see that angular momentum is transferred outwards (positive flux) since waves in $r > r_{\text{OL}}$ carries positive angular momentum. For Region I we have [up to the same proportional constant as in (69)]

$$\delta h = \sqrt{S/k} \left[\exp \left(-i \int_{r_{\text{IL}}}^r k dr + \frac{\pi}{4} \right) + \mathcal{R} \exp \left(i \int_{r_{\text{IL}}}^r k dr - \frac{\pi}{4} \right) \right], \quad (71)$$

which gives the angular momentum flux:

$$F(r \ll r_{\text{IL}}) \simeq \pi m (|\mathcal{R}|^2 - 1). \quad (72)$$

We see that the incident wave carries negative angular momentum outward, and the reflected wave transfers positive angular momentum. The net angular momentum transfer is positive (in the outward direction) for $|\mathcal{R}| > 1$.

Now consider the angular flux near the corotation radius, at $r = r_c^-$ (just inside corotation) and at $r = r_c^+$ (just outside corotation). Integrating equation (36) across the singularity, we find the discontinuity in the enthalpy perturbation derivatives:

$$\left. \frac{d\delta h}{dr} \right|_{r_c^+} - \left. \frac{d\delta h}{dr} \right|_{r_c^-} = \frac{2\pi i}{q} \left(\frac{d}{dr} \ln \zeta \right) \delta h \Big|_{r_c} = 2\pi \nu i \frac{\kappa}{c} \delta h \Big|_{r_c}. \quad (73)$$

Here we have chosen to integrate from r_c^- to r_c^+ by going through the upper complex plane, to be consistent with the physical requirement of a gradually growing perturbation, turned on at $t = -\infty$. Thus the change in the angular momentum flux across the corotation is

$$\Delta F_c = F(r_c^+) - F(r_c^-) = -\frac{2\pi^2 m r \Sigma \nu \kappa}{c D} |\delta h|^2 \Big|_{r_c}. \quad (74)$$

The wavefunction around r_c is given by equation (57) multiplied by \mathcal{T} . Noting that

$$\psi_-(r_c) = W_{\nu, 1/2}(0) = \frac{1}{\Gamma(1-\nu)}, \quad (75)$$

$$\psi_+(r_c) = e^{-i\pi\nu} W_{-\nu, 1/2}(0) + \frac{1}{2} T_0 W_{\nu, 1/2}(0) = \frac{\cos \pi \nu}{\Gamma(1+\nu)}, \quad (76)$$

where we have used the convenient identity $\Gamma(\nu)\Gamma(1-\nu) = \pi/\sin \pi\nu$. We can evaluate the enthalpy perturbation at the corotation, giving

$$\delta h(r_c) = \sqrt{S/k} \mathcal{T} \left[\frac{1}{2} e^{-\Theta_{\text{Ib}}} \frac{\cos \pi \nu}{\Gamma(1+\nu)} + i e^{\Theta_{\text{Ib}}} \frac{1}{\Gamma(1-\nu)} \right]. \quad (77)$$

The change in angular momentum flux across the corotation is then

$$\Delta F_c = -\pi m |\mathcal{T}|^2 \nu \left[\frac{\pi}{2} \frac{\cos^2 \pi \nu}{(\Gamma(1+\nu))^2} e^{-2\Theta_{\text{Ib}}} + \frac{2\pi}{(\Gamma(1-\nu))^2} e^{2\Theta_{\text{Ib}}} \right]. \quad (78)$$

With $F(r \ll r_{\text{IL}}) = F(r_c^-)$, $F(r \gg r_{\text{OL}}) = F(r_c^+)$, and thus $F(r \ll r_{\text{IL}}) = F(r \gg r_{\text{OL}}) - \Delta F_c$, we find

$$\mathcal{D}_c = |\mathcal{T}|^2 \nu \left[\frac{\pi}{2} \frac{\cos^2 \pi \nu}{(\Gamma(1+\nu))^2} e^{-2\Theta_{\text{Ib}}} + \frac{2\pi}{(\Gamma(1-\nu))^2} e^{2\Theta_{\text{Ib}}} \right]. \quad (79)$$

This expression exactly agrees with \mathcal{D}_c given in section 4.2.

6 RESULTS AND DISCUSSION

The key new results of this paper consist of the analytical expressions for the reflection coefficient \mathcal{R} , transmission coefficient \mathcal{T} and the dissipation term \mathcal{D}_c when a wave impinges upon the corotation barrier from small radii. These expressions, (61)-(66) and (79), can be applied to discs with generic rotation and surface density profiles.

For definiteness, here we illustrate our results using a (Newtonian) Keplerian disc model with

$$\Omega = \kappa \propto r^{-3/2}, \quad \Sigma \propto r^{-p}, \quad \frac{c}{r\Omega} = \beta, \quad (80)$$

where p and β are constants. The important parameter that determines the behavior of the corotation singularity is [see eq. (40)]

$$\nu = \left(\frac{2c}{3\kappa} \frac{d}{dr} \ln \zeta \right)_c = \frac{2}{3} \beta \left(p - \frac{3}{2} \right). \quad (81)$$

Clearly the models are scale-free, and \mathcal{R} , \mathcal{T} and \mathcal{D}_c depend only on the two parameters p and β (or ν). Figure 4 depicts $|\mathcal{R}|$ as a function of β for different values of p , while Figure 5 shows $|\mathcal{R}|$, \mathcal{D}_c and $|\mathcal{T}|$ as a function of ν for $\beta = 0.05$ and $\beta = 0.1$.

A key result of paper is that wave absorption at the corotation resonance plays an important role in determining the reflection and transmission of waves across the corotation barrier. Without corotation resonance (as for discs with zero vortensity gradient, or $\nu = 0$), super-reflection is always achieved, but $|\mathcal{R}|^2 - 1 \simeq \exp(-2\Theta_{\text{II}})$ (assuming $\Theta_{\text{II}} \gg 1$, where $\Theta_{\text{II}} = \Theta_{\text{IIa}} + \Theta_{\text{IIb}} = \int_{r_{\text{IL}}}^{r_{\text{OL}}} |k| dr$, with $|k| = |D|^{1/2}/c$) is rather small. In the presence of wave absorption at the corotation resonance (when $\nu \neq 0$), we find (assuming $\Theta_{\text{IIa}} \gg 1$ and $|\nu| \ll 1$),

$$|\mathcal{R}|^2 - 1 \simeq \exp(-2\Theta_{\text{II}}) + 2\pi\nu \exp(-2\Theta_{\text{IIa}}), \quad (82)$$

and super-reflection can be much more prominent. From Fig. 5 we see that the transmission coefficient is generally much smaller than \mathcal{D}_c . Thus the reflectivity depends mainly on the wave damping at corotation.

Equation (79) or (66) clearly shows that for $\nu > 0$, the wave damping term due to corotation resonance is positive, $\mathcal{D}_c > 0$. This can be understood from the fact that for $\nu > 0$ the Rossby wave region lies outside r_c (see Fig. 3), and the dissipation at the corotation singularity carries away positive energy (just like the transmitted wave) so that energy conservation [see eq. (46)] requires $-1 = -|\mathcal{R}|^2 + |\mathcal{T}|^2 + |\mathcal{D}_c|$. In this case the corotation singularity enhances super-reflection, as seen in Figs. 4-5. On the other hand, for $\nu < 0$, the Rossby wave zone lies inside r_c (Fig. 2) and the dissipation carries away negative

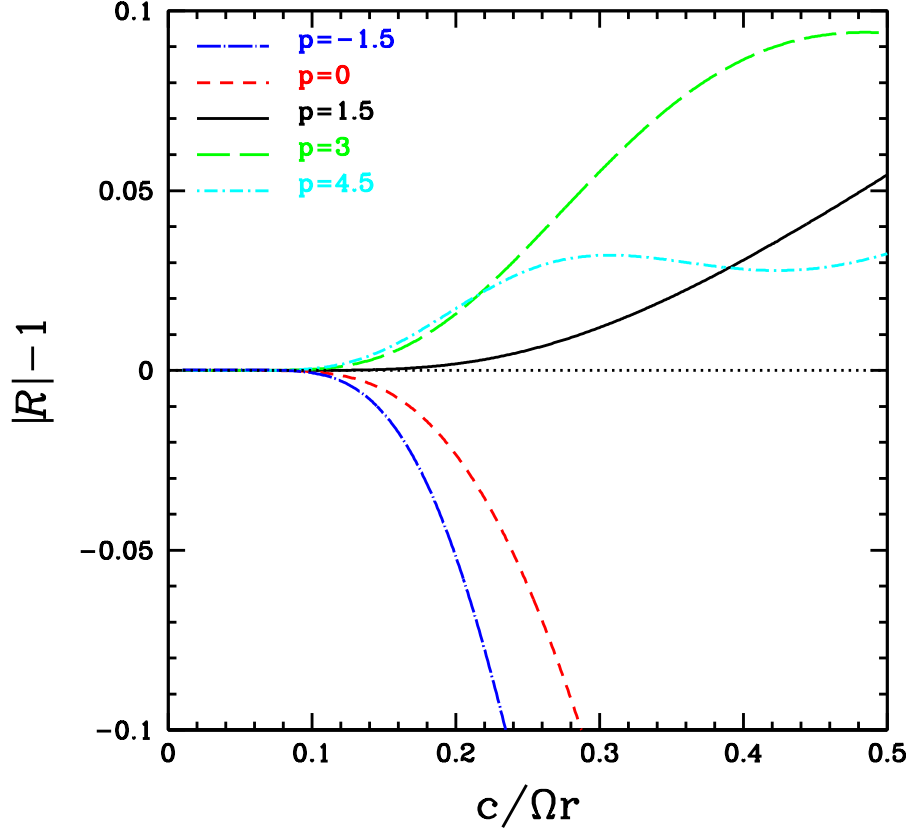


Figure 4. The reflection coefficient as a function of $\beta = c/(r\Omega)$ for Keplerian discs with surface density profile $\Sigma \propto r^{-p}$. Note that for $p = 1.5$, wave absorption at the corotation resonance is absent.

energy (like the reflected wave) so that $-1 = -|\mathcal{R}|^2 + |\mathcal{T}|^2 - |\mathcal{D}_c|$. In this case the corotation singularity tends to reduce super-reflection, and there is a competition between the effect of the corotation amplifier [the first term in eq. (64)] and the effect of the corotational absorption [the second term]. To obtain $|\mathcal{R}| > 1$ we require

$$\nu > -\frac{1}{2\pi} \frac{1 - \frac{1}{4}e^{-2\Theta_{\text{Ib}}}}{e^{2\Theta_{\text{Ib}}} - \frac{1}{4}e^{-2\Theta_{\text{Ib}}}} \simeq -\frac{1}{2\pi} e^{-2\Theta_{\text{Ib}}}, \quad (83)$$

where the second inequality applies in the limit of $\Theta_{\text{Ib}} \gg 1$. This puts a constraint on the disc thickness and the specific vorticity slope (note that the sound speed c enters into both ν and Θ_{Ib}) in order to achieve super-reflection. For example, for a given c , the inequality (83) determines the critical value of p for which $|\mathcal{R}| = 1$.

Figures 4-5 also reveal an intriguing oscillatory behavior of the reflection, transmission and damping coefficients. This non-monotonic behavior may be qualitatively understood from the Rossby wave zone around r_c (see Figs. 2-3). The WKB wavenumber k_r in the near vicinity of r_c is given by

$$k_r^2 \simeq -\frac{\kappa^2}{c^2} + \frac{2m\Omega}{r\tilde{\omega}} \frac{d}{dr} \ln \zeta = \frac{\kappa^2}{c^2} \left(-1 + \frac{2\beta\nu r}{r - r_c} \right). \quad (84)$$

For $\nu > 0$, the Rossby wave zone lies between r_c and $r_c + \Delta r_R$, where $\Delta r_R = 2\beta\nu r_c$. For quasi-normal modes to be “trapped in” the Rossby wave zone they must obey the Sommerfeld “quantization” condition⁶ $\int_{r_c}^{r_c + \Delta r_R} dr k_r = \pi\nu \sim n\pi + \pi/2$, where $n = 0, 1, 2, \dots$. Thus when $\nu \simeq n + 1/2$, the wave propagating in the Rossby zone (Fig. 3) is maximally reflected back to the singularity, leading to maximum negative damping and enhanced net reflection, as seen in Fig. 5. For $\nu < 0$ the Rossby wave zone lies between $r_c - |\Delta r_R|$ and r_c (Fig. 2), the wave in the Rossby zone is mostly absorbed at the corotation singularity. The asymmetry in the $\nu > 0$ case and the $\nu < 0$ case can also be seen in the toy problem of resonant tunneling (Appendix B). Note that for thin Keplerian disks, $|\nu|$ is much less than unity for reasonable density profiles ($|p| \sim 1$), so this non-monotonic behavior is of no practical interest.

⁶ The phase factor $\pi/2$ arises from a detailed analysis of the wave behavior at $r = r_c$ and at $r = r_c + \Delta r_R$: The former gives a phase of $-3\pi/4$ and the latter gives $\pi/4$.

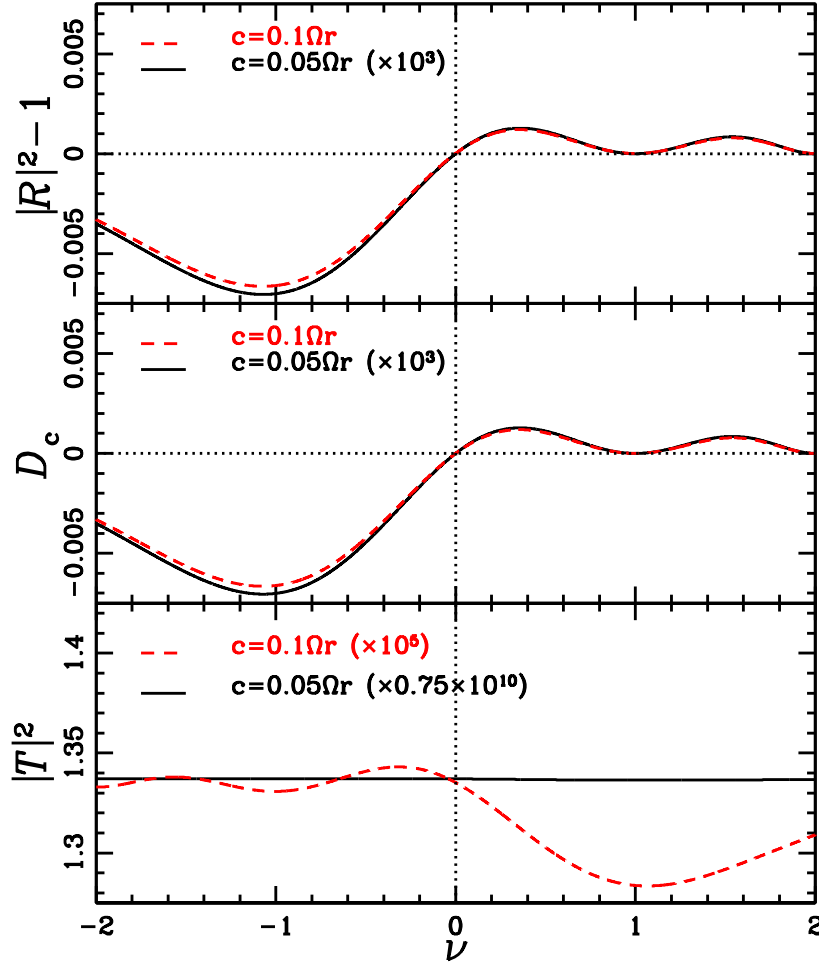


Figure 5. The reflection coefficient, wave damping coefficient and transmission coefficient as a function of ν for two different values of $\beta = c/(r\Omega)$. Note that for $\nu = 0$ (no corotation resonance), wave damping is zero ($D_c = 0$) and $|\mathcal{R}|^2 - 1$ is positive.

6.1 Numerical Calculation of Reflectivity and Improved WKB Treatment

Our analytical expressions derived in section 4-5 are based on global WKB analysis and involves several approximations. In particular, in our treatment of the corotation resonance (section 3.2), we assumed $c \ll r\Omega$ — if this is not satisfied, some of the neglected terms must be included in equation (36) and the numerical values of our solution may be modified. Thus our results for $\beta \gtrsim 0.1 - 0.2$ should be treated with caution.

To assess the validity of our WKB analysis, we also carry out computation of the reflectivity by numerical integration of equations (8)-(10). The outgoing wave boundary condition, equation (48), is imposed at some radius $r_{\text{out}} \gg r_{\text{OL}}$, such that

$$\delta h' = \left(ik + \frac{S'}{2S} - \frac{k'}{2k} \right) \delta h, \quad (85)$$

where $'$ specifies derivatives with respect to r . At some inner radius $r_{\text{in}} \ll r_{\text{IL}}$, the solution takes the form of equation (71). The reflection coefficient can be obtained from

$$|\mathcal{R}| = \left| \frac{\left[\left(\frac{S'}{2S} - \frac{k'}{2k} \right) - ik \right] \delta h - \delta h'}{\left[\left(\frac{S'}{2S} - \frac{k'}{2k} \right) + ik \right] \delta h - \delta h'} \right|_{r_{\text{in}}} \quad (86)$$

while the transmission is

$$|\mathcal{T}| = \left| \frac{2k}{\left[\left(\frac{S'}{2S} - \frac{k'}{2k} \right) + ik \right] \delta h - \delta h'} \right|_{r_{\text{in}}} |\delta h|_{r_{\text{out}}} . \quad (87)$$

Because of the singularity at corotation, we include a small positive $\omega_i = \text{Im}(\omega)$ for the frequency so that singularity can be avoided. Figure 6 depicts an example calculation for a Keplerian disc with $\beta = 0.1$ and $p = 2$ (so that $\nu = 0.033$).

Figure 7 shows our numerical result compared with the calculation from the WKB analysis. There is qualitative agreement

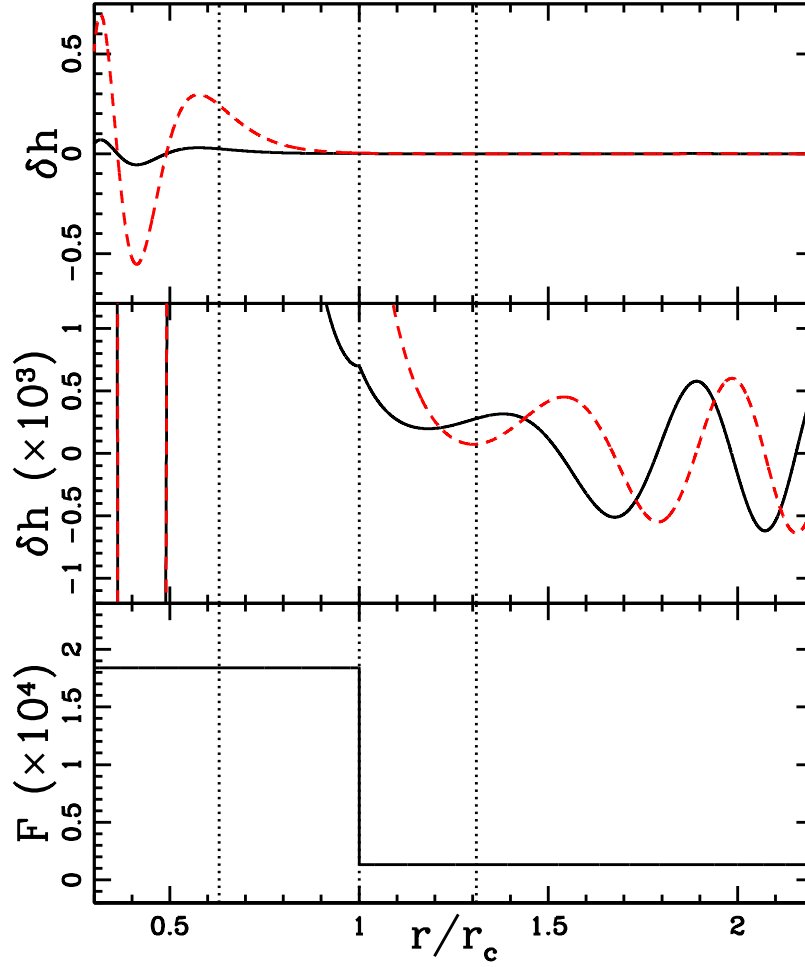


Figure 6. Numerical calculation of wave reflection and transmission across corotation for a Keplerian disc with $\nu = 0.033$ and $\beta = 0.1$. The top and middle panel show the enthalpy perturbation δh , with the solid lines depicting the real components and the dashed lines the imaginary components. Note that there is a discontinuity in the derivative of δh at the corotation resonance, resulting in an absorption of flux at the corotation. The bottom panel shows the angular momentum flux carried by the wave [see eq. (67)]. Note that $F(r)$ is conserved away from corotation and the discontinuity in F at $r = r_c$ results from wave absorption. The Lindblad and corotation resonances are indicated by three vertical dotted lines.

between these results. In particular, both the numerical and WKB results show that wave absorption at corotation plays the dominant role in determining $|\mathcal{R}|$, and wave transmission is unimportant even for small (but nonzero) ν .

However, the WKB solution matches the numerical result closely only for $|\nu| \ll 1$, indicating that our WKB analysis can be improved. For the Keplerian disc considered here, the variation in ν was achieved by changing the background density index p . The WKB results shown in Figs. 5-6 assume that the quantities Θ_{IIa} and Θ_{IIb} are not effected by changing ν . However p plays a non-negligible role in determining the effective wave number away from the corotation and Lindblad resonances. Indeed, in obtaining equation (22) or (36) from (15), we have neglected several terms that are negligible near r_c or $r_{\text{IL/OL}}$, but nevertheless important away from these resonances. Noting that our connection formulae [equations (32)-(35) and (42)-(43)] involve the asymptotic expansions of local solutions around the resonances, we can improve our WKB results by adopting the following ansatz: we modify the integrands in Θ_{IIa} and Θ_{IIb} to include these dropped terms,

$$\Theta = \int \sqrt{-k_{\text{eff}}^2} dr, \quad (88)$$

$$k_{\text{eff}}^2 = -\frac{D}{c^2} - \frac{m^2}{r^2} - \frac{p^2 - 1}{4r^2} - D^{1/2} \left(\frac{d}{dr} D^{-1/2} \right) \frac{1-p}{2}. \quad (89)$$

Note that in the expression above, we have left out the singular term ($\propto \tilde{\omega}^{-1}$) at corotation and the dominant double singular term ($\propto D^{-2}$) at the Linblad resonances since they have already been accounted for by the connection formulae in sections 3. As shown in Fig. 6, the improved WKB result matches the numerical solution for a much larger range of ν . The increased values of Θ_{IIa} and Θ_{IIb} for larger $|p|$ act to suppress super-reflection, and drive reflection coefficient toward $|\mathcal{R}| = 1$.

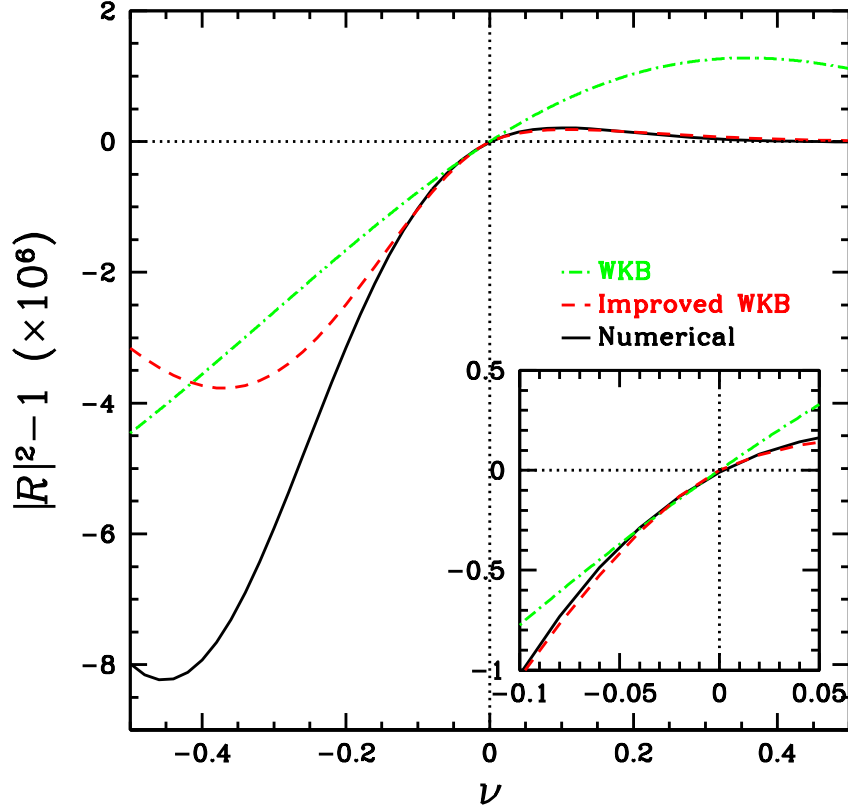


Figure 7. The reflection coefficient as a function of ν calculated using the WKB, improved WKB, and numerical methods for a scale free Keplerian disk with sound speed $c = 0.05\Omega r$.

7 GLOBAL OVERSTABLE MODES

As mentioned in Section 1, global disc instabilities are often related to the super-reflection at the corotation barrier. To illustrate this, we consider a simple boundary condition

$$\delta h(r_{\text{in}}) = 0 \quad (90)$$

at the inner radius of the disc, $r_{\text{in}} \ll r_{\text{IL}}$. The outgoing boundary condition at $r > r_{\text{OL}}$ implies that the solution in the region $r < r_{\text{IL}}$ is given by

$$\delta h = \sqrt{S/k} \exp\left(-i \int_{r_{\text{IL}}}^r k dr + \pi/4\right) + \mathcal{R} \sqrt{S/k} \exp\left(i \int_{r_{\text{IL}}}^r k dr - \pi/4\right). \quad (91)$$

Letting $\mathcal{R} = |\mathcal{R}|e^{i\varphi}$, and applying the boundary condition (91) yields the eigenvalue condition:

$$\tan\left(\int_{r_{\text{in}}}^{r_{\text{IL}}} k dr - \pi/4 - \varphi/2\right) = -i \left(\frac{|\mathcal{R}| - 1}{|\mathcal{R}| + 1}\right). \quad (92)$$

Noting that for complex eigenvalue $\omega = \omega_r + i\omega_i$, the wavenumber k is also complex

$$k = k_r + ik_i = \frac{1}{c} \sqrt{(\tilde{\omega}_r + i\tilde{\omega}_i)^2 - \kappa^2} \simeq \frac{1}{c} \sqrt{\tilde{\omega}_r^2 - \kappa^2} + i \frac{\omega_i \tilde{\omega}_r}{c \sqrt{\tilde{\omega}_r^2 - \kappa^2}}, \quad (93)$$

where we have assumed $|\omega_i| \ll |\omega_r|$. $\tilde{\omega}_r = \omega_r - m\Omega$ (< 0 for region I) and thus the real part of the eigenvalue condition gives

$$\int_{r_{\text{in}}}^{r_{\text{IL}}} \frac{1}{c} \sqrt{(\omega_r - m\Omega)^2 - \kappa^2} dr - \pi/4 - \varphi/2 = n\pi, \quad (94)$$

where n is an integer. The imaginary part of (92) gives (assuming $|k_i| \ll |k_r|$)

$$\int_{r_{\text{in}}}^{r_{\text{IL}}} k_i dr \simeq - \left(\frac{|\mathcal{R}| - 1}{|\mathcal{R}| + 1}\right), \quad (95)$$

from which we find the growth rate

$$\omega_i = \left(\frac{|\mathcal{R}| - 1}{|\mathcal{R}| + 1} \right) \left[\int_{r_{\text{in}}}^{r_{\text{TL}}} |\tilde{\omega}_r| / c \sqrt{\tilde{\omega}_r^2 - \kappa^2} dr \right]^{-1}. \quad (96)$$

Thus the modes are overstable ($\omega_i > 0$) for $|\mathcal{R}| > 1$, and stable ($\omega_i < 0$) for $|\mathcal{R}| < 1$.

8 CONCLUSION

In this paper we have derived explicit expressions for the reflection coefficient, transmission coefficient and wave absorption coefficient when a wave is scattered by the corotation barrier in a disc. These expressions include both the effects of corotation amplifier (which exists regardless of the gradient of the vortensity $\zeta = \kappa^2/\Omega\Sigma$ of the background flow) and wave absorption at the corotation (which depends on $d\zeta/dr$). They demonstrate clearly that the corotation wave absorption plays a dominant role in determining the reflectivity and that the sign of $d\zeta/dr$ determines whether the corotation singularity enhances or diminishes the super-reflectivity. Our result can be understood in terms of the location of the Rossby wave zone relative to the corotation radius. We also carried out numerical calculations of the reflectivity. Our result provides the conditions (in terms of disc thickness, rotation profile and surface density profile) for which super-reflection is achieved and global overstable modes in discs are possible.

In future works we will explore global oscillation modes and their stabilities in a variety of astrophysical contexts, ranging from accreting white dwarfs to accreting black hole systems. The possible overstabilities of these modes are directly linked to the effects studied in this paper and may provide explanations for some of the quasi-periodic variabilities observed in these systems.

ACKNOWLEDGMENTS

DL thanks Peter Goldreich and Ramesh Narayan for useful conversations. This work has been supported in part by NASA Grant NNX07AG81G, NSF grants AST 0707628, and by *Chandra* grant TM6-7004X (Smithsonian Astrophysical Observatory).

APPENDIX A: STOKES PHENOMENON AND THE MATCHING CONDITION ACROSS THE COROTATION SINGULARITY

As we saw in section 3.1 the perturbation equation near the corotation resonance can be solved in terms of the Whittaker function. However in order to provide the matching conditions we must carefully consider the effect of the Stokes Phenomenon on the asymptotic expansions.

Stokes phenomenon causes the functional form of the asymptotic expansion of an entire function to be different at different points in the complex plane. The general asymptotic solution of the Whittaker equation for $|z| \gg 1$ can be written as a linear combination of two functions

$$P(z) = e^{z/2} z^{-\nu}, \quad Q(z) = e^{-z/2} z^{\nu}, \quad (\text{A-1})$$

i.e., $AP(z) + BQ(z)$. However, because of the Stokes phenomenon, the coefficients A and B can change when crossing the Stokes lines. For Whittaker functions, the Stokes lines are the positive real axis (where P is dominant and Q is sub-dominant) and negative real axis (where Q is dominant and P is sub-dominant).

Consider specific solution to the Whittaker equation, with the asymptotic expansion ($|z| \gg 1$) given by

$$F(z) \rightarrow AP(z) + BQ(z), \quad (\text{for } \arg(z) = 0) \quad (\text{A-2})$$

on the real axis. Our goal is to derive the expansion coefficients of $F(z)$ on the negative real axis ($\arg(z) = \pi$). To achieve this, we use the general results obtained by Heading (1962):

(1) “The coefficient of the subdominant term after crossing the Stokes line = the coefficient of the subdominant term before crossing the Stokes line + $T_n \times$ the coefficient of the dominant term on the Stokes line.”

(2) “The coefficient of the subdominant term on the Stokes line = the coefficient of the subdominant term before the Stokes line + $\frac{1}{2}T_n \times$ the coefficient of the dominant term on the Stokes line.”

Here T_n is the Stokes multiplier for crossing the Stokes line $\arg(z) = n\pi$ in the direction of increasing $\arg(z)$ given by ⁷

$$T_n = \frac{2\pi i e^{-2\pi i n s \nu}}{\Gamma(s\nu)\Gamma(1+s\nu)} \quad (\text{A-3})$$

⁷ Note that a typo in equation (18) of Heading (1962) has been corrected here.

where $s = (-1)^n$. Note that since the pole of equation (39) lies below the real axis, $\arg(z)$ increases as we move along the contour from z positive and real ($\arg(z) = 0$) to z negative and real ($\arg(z) = \pi$).

Since equation (A-2) is given on one of the Stokes line, we first determine $F(z)$ in the region $-\pi < \arg(z) < 0$:

$$F(z) \sim AP(z) + \left(B - \frac{1}{2}T_0A\right)Q(z), \quad (\text{for } -\pi < \arg(z) < 0). \quad (\text{A-4})$$

Then in region $0 < \arg(z) < \pi$ we have

$$F(z) \sim AP(z) + \left(B + \frac{1}{2}T_0A\right)Q(z), \quad (\text{for } 0 < \arg(z) < \pi). \quad (\text{A-5})$$

Thus on the negative real axis, we obtain

$$F(z) \sim \left[A + \frac{1}{2}T_1\left(B + \frac{1}{2}T_0A\right)\right]P(z) + \left(B + \frac{1}{2}T_0A\right)Q(z), \quad (\text{for } \arg(z) = \pi). \quad (\text{A-6})$$

The connection formulae for the two independent Whittaker functions for $|z| \gg 1$ are

$$\psi_- = W_{\nu, 1/2}(z) \sim \begin{cases} Q(z) & \arg(z) = 0 \\ Q(z) + \frac{1}{2}T_1P(z) & \arg(z) = \pi \end{cases} \quad (\text{A-7})$$

$$\psi_+ = e^{-i\pi\nu}W_{-\nu, 1/2}(ze^{-i\pi}) + \frac{1}{2}T_0W_{\nu, 1/2}(z) \sim \begin{cases} P(z) & \arg(z) = 0 \\ \frac{1}{2}T_0Q(z) + (1 + \frac{1}{4}T_0T_1)P(z) & \arg(z) = \pi, \end{cases} \quad (\text{A-8})$$

where $P(z)$ and $Q(z)$ have the asymptotic behavior

$$P(z) = e^{+z/2 - \nu \log(z)} \sim \begin{cases} \exp\left(\int_{r_c}^r \tilde{k} dr\right) & \text{for } r \gg r_c \\ e^{-i\pi\nu} \exp\left(-\int_r^{r_c} \tilde{k} dr\right) & \text{for } r \ll r_c. \end{cases} \quad (\text{A-9})$$

$$Q(z) = e^{-z/2 + \nu \log(z)} \sim \begin{cases} \exp\left(-\int_{r_c}^r \tilde{k} dr\right) & \text{for } r \gg r_c \\ e^{i\pi\nu} \exp\left(\int_r^{r_c} \tilde{k} dr\right) & \text{for } r \ll r_c. \end{cases} \quad (\text{A-10})$$

for $|z| \gg 1$, since in this limit $|z| \gg \log|z|$.

APPENDIX B: RESONANCE TUNNELING

To help understand the effect of wave absorption at the corotation singularity we consider the following toy problem. For a 1-D quantum mechanical potential of the form

$$V(x) = \frac{C}{x}, \quad (\text{B-1})$$

we have the time-independent wave equation

$$\left(\frac{1}{2} \frac{d^2}{dx^2} + E - \frac{C}{x + i\epsilon}\right) \psi = 0, \quad (\text{B-2})$$

where we have set the Planck constant and particle mass to unity. In equation (B-2), a small imaginary part $i\epsilon$ is added to x , to account for the physical requirement of a growing incoming perturbation. The sign of ϵ must be the same as the sign of C , so as to give us the correct physical behavior. For concreteness we will assume $C > 0$ (and thus $\epsilon > 0$), though the same calculation can be performed for $C < 0$ ($\epsilon < 0$) with similar results.

Let $y = 2ik(x + i\epsilon)$, where $k = \sqrt{2E}$, we have

$$\frac{d^2\psi}{dy^2} + \left(-\frac{1}{4} + \frac{\nu}{y}\right) \psi = 0, \quad \text{with } \nu = iC/k, \quad (\text{B-3})$$

which we recognize as the Whittaker differential equation. With $C > 0$, y lies in the domain $\pi/2 \leq \arg(y) \leq 3\pi/2$. Using the same procedure as discussed in Appendix A, we obtain the connection formulae for the general solution of equation (B-3) as

$$\psi \rightarrow \begin{cases} AP(z) + BQ(z) & \text{for } \arg(z) = \pi/2 \\ (A + T_1B)P(z) + BQ(z) & \text{for } \arg(z) = 3\pi/2. \end{cases} \quad (\text{B-4})$$

Consider a wave propagating from $x = -\infty$ and impinging on the potential. The transmitted wave at $x > 0$ has the form

$$\psi_+ \rightarrow e^{y/2} y^{-\nu} = e^{ikx - i(C/k) \ln|2kx| + \pi C/2k} \quad \text{for } x \gg 1/k. \quad (\text{B-5})$$

The corresponding wave solution in the $x < 0$ region has the asymptotic form

$$\psi_+ \rightarrow e^{y/2} y^{-\nu} = e^{ikx - i(C/k) \ln|2kx| + 3\pi C/2k} \quad \text{for } x \ll -1/k. \quad (\text{B-6})$$

This gives

$$|\mathcal{R}| = 0, \quad |\mathcal{T}| = e^{-\pi C/k} \quad (\text{B-7})$$

for a wave incident from $x < 0$.

Now consider a wave incident from the $x > 0$ region towards small x . The transmitted wave is given by

$$\psi_- \rightarrow e^{-y/2} y^{+\nu} = e^{-ikx+i(C/k)\ln|2kx|-3\pi C/2k} \quad \text{for } x \ll -1/k. \quad (\text{B-8})$$

Connecting to the $x > 0$ region, we have

$$\psi_- \rightarrow e^{-y/2} y^{+\nu} - T_1 e^{y/2} y^{-\nu} = e^{-ikx+i(C/k)\ln|2kx|-\pi C/2k} - T_1 e^{ikx-i(C/k)\ln|2kx|+\pi C/2k} \quad \text{for } x \gg 1/k. \quad (\text{B-9})$$

This gives the reflection and transmission coefficients

$$|\mathcal{R}| = e^{\pi C/k} |T_1| = \frac{2\pi e^{-\pi C/k}}{|\Gamma(-iC/k)\Gamma(1-iC/k)|} = 2e^{-\pi C/k} \sinh(\pi C/k) = 1 - e^{-2\pi C/k}, \quad (\text{B-10})$$

$$|\mathcal{T}| = e^{-\pi C/k}, \quad (\text{B-11})$$

for a wave incident from the positive side of the singularity [a similar result was obtained by Budden (1979) in the context of wave propagation in cold plasma].

We can define the wave absorption coefficient at the singularity as

$$\mathcal{D} = 1 - |\mathcal{T}|^2 - |\mathcal{R}|^2 \quad (\text{B-12})$$

For the forward moving incident wave (+) and the backwards moving incident wave (−), we have

$$\mathcal{D}_+ = 1 - e^{-2\pi C/k}, \quad \mathcal{D}_- = e^{-2\pi C/k} (1 - e^{-2\pi C/k}). \quad (\text{B-13})$$

REFERENCES

- Abramowitz, M, Stegun, I.A. 1964, Handbook of Mathematical Functions (Dover: New York)
- Balbus, S.A., Hawley, J.F. 1998, Rev. Mod. Phys., 70, 1.
- Budden, K.G., Phil. Trans. R. Soc. Lond. A, 1979, 290, 405
- Dickenson, R.E., 1968, J. Atmos. Sci., 25, 984
- Goldreich, P. 1988, in “Origin, structure and evolution of galaxies” (Proceedings of the Guo Shoujing Summer School of Astrophysics, Tunxi, China), ed. L.Z. Fang (World Scientific: Singapore), p. 127
- Goldreich, P., Lynden-Bell, D. 1965, MNRAS, 130, 125
- Goldreich, P., Goodman, J., Narayan, R. 1986, MNRAS, 221, 339
- Goldreich, P., Tremaine, S. 1979, ApJ, 233, 857
- Goodman, J., Evans, N. 1999, MNRAS, 309, 599
- Heading, J. 1962, J. Lond. Math. Soc., 37, 195
- Julian, W.H., Toomre, A. 1966, ApJ, 146, 810
- Kato, S., 2003, PASJ, 55, 257
- Li, H., Finn, J.M., Lovelace, R.V.E., Colgate, S.A. 1999, ApJ, 533, 1023
- Li, L., Goodman, J., Narayan, R., 2003, ApJ, 593, 980
- Lin, C.C., Lau, Y.Y. 1975, SIAM J. Appl. Math., 29, 352
- Lovelace, R.V.E., Li, H., Colgate, S.A., Nelson, A.F. 1999, ApJ, 513, 805
- Lynden-Bell, D., Kalnajs, A.J. 1972, MNRAS, 157, 1
- Mark, J.W.K. 1976, ApJ, 205, 363
- Narayan, R., Goldreich, P., Goodman, J. 1987, MNRAS, 228, 1
- Papaloizou, J.C.B., Lin, D.N.C. 1995, ARAA, 33, 505
- Papaloizou, J.C.B., Pringle, J.E. 1984, MNRAS, 208, 721
- Papaloizou, J.C.B., Pringle, J.E. 1987, MNRAS, 225, 267
- Pedlosky, J. 1987, Geophysical Fluid Dynamics. Springer-Verlag, Berlin
- Shu, F.H. 1992, The Physics of Astrophysics II: Gas Dynamics. University Science Books, Mill Valley, CA, chapter 12
- Shu, F.H., Laughlin, G., Lizano, S., Galli, D., 2000, ApJ, 535, 190
- Tagger, M., Pellat, R. 1999, A&A, 349, 1003
- Tagger, M., 2001 A&A, 380, 750
- Tagger, M., Varniere, P. 2006, ApJ, 652, 1457
- Tanaka, H., Takeuchi, T., Ward, W.R. 2002, ApJ, 565, 1257
- Zhang, H., Lai, D., MNRAS, 2006, 368, 917